AIAA JOURNAL
Vol. 38, No. 7, July 2000

New Two-Equation Eddy Viscosity Transport Model for Turbulent Flow Computation

Shia-Hui Peng* and Lars Davidson†
Chalmers University of Technology, 412 96 Gothenburg, Sweden

A two-equation turbulence model is proposed in which the turbulent eddy viscosity is not constructed from scale-determining quantities but rather is calculated from a transport equation. To close the equation system while not involving a length scale as in some one-equation models, the turbulent kinetic energy is also solved as a supplemental quantity. The eddy viscosity transport equation is modeled on the basis of an exact form derived from the exact k and ε equations. The model allows integration over the near-wall region, requiring neither wall functions as a bridge nor wall distance parameters in the model coefficients. In contrast to the conventional k–ε model, moreover, natural boundary conditions can be used at the wall for the turbulent transport quantities. It is numerically convenient to use the model for computing complex turbulent flows. The model is validated against several flow cases, yielding predictions in good agreement with experimental and direct numerical simulation data.

Nomenclature

C	= model constant with various subscripts
C_f	= skin-friction coefficient
f_μ	= damping function
H	= height of the computational domain
h	= height of the hill or the step
k	= turbulent kinetic energy
Re	= Reynolds number based on freestream velocity
Re_τ	= Reynolds number based on friction velocity
R_t	= turbulent Reynolds number, $\tilde{\nu}_t / \nu$
t	= time
U, V	= Cartesian components of mean velocity
u, v	= Cartesian components of velocity fluctuation
u_τ	= friction velocity
X_r	= reattachment length
x, y	= Cartesian body axes
δ_{ij}	= Kronecker delta
ε	= dissipation rate of k
κ	= von Kármán constant
ν	= molecular kinematic viscosity
ν_t	= turbulent eddy viscosity
$\tilde{\nu}_t$	= working quantity for ν_t
σ_k, σ_t	= model constants
τ	= turbulent time scale
τ_{ij}	= Reynolds stress tensor
ω	= specific dissipation rate of k

Subscripts

c	= centerline or freestream
in	= inlet

Superscript

$+$	= normalized quantity by inner variables

I. Introduction

TURBULENCE modeling has long been and will remain one of the main topics in the turbulence research community. Great effort has been made to model (appropriately in physics and mathematics) the unknown correlation in the Reynolds-averaged Navier–Stokes (RANS) equations. These unknown terms, stemming from the Reynolds decomposition, are usually expressed with constitutive relations using either the eddy viscosity concept or modeled transport equations. Over the past few years, approaches more advanced than the RANS modeling have gained increasing popularity with the rapid development of digital computers, such as direct numerical simulation (DNS) and large eddy simulation (LES). Although DNS is able to provide desirable details on the turbulence structure and give accurate simulations, its requirements on computational resources are still prohibitive at present for solving engineering flow problems at high Reynolds numbers, whereas LES has attracted relatively extensive studies and implementations. The physical rationale behind LES is more plausible than RANS modeling because the filtered large-scale motion is resolved and the effect of subgrid scales is said to be more isotropic and less dependent on flow boundaries. Subgrid-scale (SGS) modeling can consequently be expected to be more universal in physics than RANS modeling. Despite such advantages, the current LES technique cannot yet be viewed as a universal approach to handling different flows. Furthermore, the grid resolution used in LES may be coarser than in DNS but must still be sufficiently fine for the filtering cutoff to benefit from the inertial-subrange mechanics in SGS modeling. The numerical solution for flow problems encountered in engineering applications still needs to rely largely on the RANS method for the time being.

Of various RANS approaches, two-equation eddy viscosity models remain the most commonly used: They have often been regarded as a favorable compromise between computational accuracy and efficiency to solve engineering flow problems. Nonetheless, high-Reynolds-number RANS models are usually not capable of properly yielding near-wall resolution where wall damping and viscous effects become significant. Abandoning the use of wall functions to patch near-wall regions, a large number of low-Reynolds-number (LRN) modifications have instead been proposed to different types of two-equation models, for example, LRN k–ε models,[1] LRN k–ω models[2,3] and LRN k–τ models.[4] In nearly all existing LRN models, empirical functions have been used to account for near-wall turbulence and often employ local wall distance parameters (e.g., y^+, R_y, etc.) and consequently complicate the computation for flows with complex geometry. In addition, the wall boundary condition for the dissipation rate ε must either be derived or postulated, introducing uncertainties into the computations.[1,4] Nonetheless, these LRN models have met with different degrees of success in validations and practical applications.

For aerodynamic flows, approaches much simpler than two-equation models, such as algebraic models, have gained historically notable success in dealing with boundary layers, e.g., the Baldwin–Lomax model[5] and the Johnson–King model.[6] As Spalart and Allmaras[7] pointed out, however, these models treat the whole

Received 12 May 1999; revision received 13 August 1999; accepted for publication 15 October 1999.

*Assistant Professor, Department of Thermo and Fluid Dynamics.
†Professor, Department of Thermo and Fluid Dynamics.

boundary layer as a single, tightly coupled module and show difficulties in the presence of detached and multiple shear layers. Alternatively, one-equation turbulence models have been employed for wall-bounded flows; see, for example, Bradshaw et al.,[8] where a transport equation for the turbulent kinetic energy is solved in conjunction with a geometry-related, empirical formulation for the length scale to determine the eddy viscosity.

Unlike the one-equation model, where the eddy viscosity is constructed with the aid of an algebraic expression for the length scale, Baldwin and Barth[9] proposed a transport equation from which this constitutive quantity is computed. The eddy viscosity transport equation is derived from the k–ε model on the basis of some assumptions for simplification. This one-equation model turns out to be attractive for computing wall-bounded aerodynamic flows without requiring an algebraic formulation for the length scale. Prompted by the Baldwin–Barth model, Spalart and Allmaras[7] developed an alternative option for the eddy viscosity equation by means of an empirical approach and through promising calibrations on two-dimensional mixing layers, wakes, and boundary layers. The Spalart–Allmaras model was constructed in a calibrating procedure by adding additional terms step by step from simple free shear flows to complicated viscous flows past solid bodies and with laminar regions. Several empirical functions were consequently introduced into the complete model equation. With equal Prantdl numbers for the diffusion terms in the modeled k and ε equations, Menter[10] transformed these two equations into a transport equation for the eddy viscosity, where the k-related term was further eliminated by the use of the Bradshaw assumption[8] to close the equation system. Menter's model is able to overcome the strong dependency on freestream values in free-shear layer computations (a weakness nestled in the Baldwin–Barth model). This model was claimed to give very similar, or, for boundary-layer flows, improved predictions when compared to its parent k–ε model from which it has been transformed, albeit possessing some similar deficiencies.

The aforementioned one-equation models based on the eddy viscosity transport equation have been developed in applications to aerodynamic flows, where mixing layers, wakes, and boundary layers are considered to be the basic flow features.[7] These models have reached some impressive success in their applications to aerodynamic flows. Their validity for internal turbulent flows has not been well calibrated, however. In the Spalart–Allmaras model, moreover, the determination of wall distance, being involved in the destruction term and model functions, may complicate the computation of geometrically complex flows. The other models transformed from the k–ε model have been constructed on the basis of some further assumptions. Until the degree of the generality of such assumptions is further verified, it is somewhat uncertain whether these models would perform better than their parent k–ε model for complex internal flows, where the k–ε model itself has been in many cases an awkward approach, motivating one to develop other model variants. Nevertheless, the development of these models sheds light on the use of an eddy viscosity transport equation for computing complex internal flows, where some flow features are in line with aerodynamic flows, such as boundary layers and flow separation. A straightforward advantage of using such models is the natural boundary condition for the eddy viscosity (being zero) both on the wall surface and in the far field.

This work presents a two-equation model in which a transport equation is constructed for the eddy viscosity. The turbulent kinetic energy is also solved as a supplemental quantity to close the equation system. Unlike one-equation models, the k equation in the present model is used mainly to avoid the determination of a length scale involved in the destruction term for the eddy viscosity. The use of an additional equation for k is affordable both physically and numerically, compared with the one-equation model, in which further assumptions are often required to eliminate or reformulate k-related terms. The present model employs only one empirical model function and does not require any local wall parameters (e.g., y^+, R_y, etc.). It is, therefore, convenient to apply it to complex turbulent flow calculations. The model is scrutinized in computations for channel flow and for flow over a hill mounted on the bottom wall of a plane channel, as well as for backward-facing step flows. The results are compared with available experimental and DNS data.

II. Model Formulation

This work considers only incompressible steady flows. The turbulent stress tensor in the time-averaged Navier–Stokes equations, stemming from the Reynolds decomposition, represents the effect of fluctuations on the mean motion or, in other words, represents the ability of turbulence to transport momentum. The linear eddy viscosity model uses the Boussinesq assumption in which the resulting Reynolds stress tensor, $\tau_{ij} = -\overline{u_i u_j}$, is modeled in alignment with the mean strain rate tensor through the eddy viscosity concept ν_t. This gives

$$\tau_{ij} - (\delta_{ij}/3)\tau_{kk} = 2\nu_t S_{ij} \tag{1}$$

where S_{ij} is the local mean strain rate tensor, reading

$$S_{ij} = \frac{1}{2}\left(\frac{\partial U_i}{\partial x_j} + \frac{\partial U_j}{\partial x_i}\right) \tag{2}$$

The closure problem then turns out to be the determination of ν_t. Dimensional reasoning suggests that $\nu_t \propto V_t L_t$, where V_t is the turbulent velocity scale and L_t is the turbulent length scale. The velocity scale is usually represented in terms of the turbulent kinetic energy with $V_t \propto \sqrt{k}$. The length scale, as in many one-equation models, may be approximated through an algebraic formulation associated with the distance to the wall surface. In two-equation models, this scale is instead constructed by using another transport equation, which is often an equation for the dissipation rate of turbulent kinetic energy ε. By definition, an exact equation for ε can be derived from the Navier–Stokes equations. The modeling of this equation is generally regarded as the most uncertain part in one-point closures. Other scale-determining quantities, together with k, can also be used to formulate ν_t, including, for example, the turbulent time scale τ (Ref. 4) and the specific dissipation rate ω (Ref. 11). The exact forms for τ and ω can be derived from the exact equations for k and ε by transformation.[4]

Apart from the two-equation models, one of the earliest one-equation models based on an eddy viscosity transport equation can be traced back to the work of Nee and Kovasznay,[12] where they assembled a transport equation for the effective viscosity $(\nu_t + \nu)$. As in some recently developed one-equation models, the Nee–Kovasznay model introduces the turbulent length scale into the destruction term originating from dimensional reasoning. Zeierman and Wolfshtein[13] derived a transport equation for a turbulent time scale τ, which is defined from the autocorrelation

$$\tau = \frac{1}{4k}\int_{-\infty}^{\infty} R_{ii}(\boldsymbol{x}, t; t')\,\mathrm{d}t' \tag{3}$$

$$\nu_t \propto k\tau = \frac{1}{4}\int_{-\infty}^{\infty} R_{ii}(\boldsymbol{x}, t; t')\,\mathrm{d}t' \tag{4}$$

where $R_{ii}(\boldsymbol{x}, t; t') = \overline{u_i(\boldsymbol{x}, t)u_i(\boldsymbol{x}, t - t')}$ is the autocorrelation for velocity fluctuations and $k = \frac{1}{2}R_{ii}(\boldsymbol{x}, t; 0)$. This enables the derivation of an exact equation for the product of $k\tau$ (proportional to ν_t) from the R_{ii} equation by integration. This exact equation contains measurable terms although, in the absence of experiments, the modeling work had to rely to a large extent on dimensional arguments.[13] The modeled $k\tau$ equation in this case turns out to have a form similar to the Nee–Kovasznay model, including a generation term, a decay term, and a diffusion term, as in other equations for transportable scalar quantities subjected to the conservation laws. Owing to the timescale definition, the Zeierman–Wolfshtein model was declared to be available only for stationary and high-Reynolds-number turbulence, from which the model constants were proposed using some simple flows without being calibrated in numerical computations for complex cases. This model was tested by the present authors for channel flows and was found to be numerically stiff and unable to give satisfactory results in its original form. On the other hand, note that Speziale et al.[4] modeled the τ equation from an exact form derived from the exact k and ε equations by transformation and reported rather encouraging results for handling near-wall turbulence.[4,14] To achieve an eddy viscosity transport model, we have thus used the transformation method rather than following Zeierman and Wolfshtein's exact $k\tau$ equation.

A. Model Equations

Instead of using the high-Reynolds-number k–ε model in the transformation, we start the derivation with the exact k and ε equations because the two are well defined through relevant mechanisms of turbulent motion. They are written, respectively, as

$$\frac{\mathrm{D}k}{\mathrm{D}t} = \mathcal{P}_k - \varepsilon - \mathcal{D}_k + \nu\nabla^2 k \tag{5}$$

$$\frac{\mathrm{D}\varepsilon}{\mathrm{D}t} = \mathcal{P}_\varepsilon - \Pi_\varepsilon - \mathcal{D}_\varepsilon + \nu\nabla^2 \varepsilon \tag{6}$$

where $\mathrm{D}/\mathrm{D}t$ denotes the substantive derivative. The terms on the right-hand side in Eqs. (5) and (6) are, respectively, the production term, the decay (dissipation) term, the turbulent diffusion term, and the viscous diffusion term. The detailed expressions for these terms can be found in the literature.[4,15] A working quantity is first defined as $\tilde{\nu}_t \propto k^2/\varepsilon$. For convenience, this quantity is termed the eddy viscosity but should be distinguished from the true eddy viscosity ν_t as it appeared in Eq. (1). The exact equation for $\tilde{\nu}_t$ can be derived from the following relation:

$$\frac{\mathrm{D}\tilde{\nu}_t}{\mathrm{D}t} = \frac{2\tilde{\nu}_t}{k}\frac{\mathrm{D}k}{\mathrm{D}t} - \left(\frac{\tilde{\nu}_t}{k}\right)^2 \frac{\mathrm{D}\varepsilon}{\mathrm{D}t} \tag{7}$$

Inserting Eqs. (5) and (6) into Eq. (7) and replacing ε in terms of k and $\tilde{\nu}_t$ yields

$$\frac{\mathrm{D}\tilde{\nu}_t}{\mathrm{D}t} = \left[\frac{2\tilde{\nu}_t}{k}\mathcal{P}_k - \left(\frac{\tilde{\nu}_t}{k}\right)^2 \mathcal{P}_\varepsilon\right] - \left[2k - \left(\frac{\tilde{\nu}_t}{k}\right)^2 \Pi_\varepsilon\right] - \left[\frac{2\tilde{\nu}_t}{k}\mathcal{D}_k - \left(\frac{\tilde{\nu}_t}{k}\right)^2 \mathcal{D}_\varepsilon\right] - \left[\mathcal{D}_\nu - \nu\nabla^2\tilde{\nu}_t\right] \tag{8}$$

In Eq. (8), the terms in square brackets on the right-hand side represent, subsequently, the production, the destruction, the turbulent diffusion, and the viscous diffusion. A part of the viscous diffusion $\mathcal{D}_\nu$ takes the form of

$$\mathcal{D}_\nu = \frac{2}{R_t}\left(\frac{\tilde{\nu}_t}{k}\frac{\partial k}{\partial x_j} - \frac{\partial \tilde{\nu}_t}{\partial x_j}\right)^2 \tag{9}$$

where the turbulent Reynolds number has been defined as $R_t = \tilde{\nu}_t/\nu$.

By the definition of $\tilde{\nu}_t$, where $\tilde{\nu}_t$ is expressed in terms of k and ε, some modeling approaches from the k–ε model may be borrowed to model the $\tilde{\nu}_t$ equation. The production term $\mathcal{P}_\varepsilon$ is modeled as

$$\mathcal{P}_\varepsilon = C_{\varepsilon 1}\frac{\varepsilon}{k}\tau_{ij}\frac{\partial U_i}{\partial x_j} = C'_{\varepsilon 1}\frac{k}{\tilde{\nu}_t}\tau_{ij}\frac{\partial U_i}{\partial x_j} \tag{10}$$

The destruction term Π_ε takes the form of

$$\Pi_\varepsilon = C_{\varepsilon 2}(\varepsilon^2/k) = C'_{\varepsilon 2}\left(k^3|\ \tilde{\nu}_t^2\right) \tag{11}$$

The turbulent diffusion for $\tilde{\nu}_t$ in Eq. (8) will not, however, be formulated by the substitution of the modeled $\mathcal{D}_k$ and $\mathcal{D}_\varepsilon$ terms from the k–ε model. It is instead modeled by the gradient-diffusion hypothesis in a form analogous to its viscous counterpart. This yields

$$\mathcal{D}_{\nu t} = -\left[\frac{2\tilde{\nu}_t}{k}\mathcal{D}_k - \left(\frac{\tilde{\nu}_t}{k}\right)^2 \mathcal{D}_\varepsilon\right] = -C_{r1}\frac{\partial\tilde{\nu}_t}{\partial x_j}\frac{\partial\tilde{\nu}_t}{\partial x_j} + C_{r2}\frac{\tilde{\nu}_t}{k}\frac{\partial\tilde{\nu}_t}{\partial x_j}\frac{\partial k}{\partial x_j} - C_{r3}\left(\frac{\tilde{\nu}_t}{k}\right)^2\frac{\partial k}{\partial x_j}\frac{\partial k}{\partial x_j} + \frac{\partial}{\partial x_j}\left(\frac{\nu_t}{\sigma_t}\frac{\partial\tilde{\nu}_t}{\partial x_j}\right) \tag{12}$$

Inspecting the viscous diffusion $\mathcal{D}_\nu$ in Eq. (9), it is obvious that this term becomes negligible for high-Reynolds-number turbulence, where $\tilde{\nu}_t \gg \nu$, that is, where $R_t \gg 1$. Even in the vicinity of a solid wall (in the viscous sublayer), this viscous diffusion part may become negligibly small owing to the small difference between $[(\tilde{\nu}_t/k)(\partial k/\partial x_j)]$ and $(\partial\tilde{\nu}_t/\partial x_j)$. We are then willing to drop $\mathcal{D}_\nu$ from the modeled $\tilde{\nu}_t$ equation for simplicity. Variable $\tilde{\nu}_t$ is viewed as a transportable turbulent quantity. It is transported by the turbulent motion as reflected in the second-order diffusion term (the last term) in Eq. (12), where the true eddy viscosity ν_t was used.

Using Eqs. (10–12) in Eq. (8), the modeled $\tilde{\nu}_t$ equation consequently takes the following form:

$$\frac{\mathrm{D}\tilde{\nu}_t}{\mathrm{D}t} = C_1\frac{\tilde{\nu}_t}{k}\tau_{ij}\frac{\partial U_i}{\partial x_j} - C_2 k + \frac{\partial}{\partial x_j}\left(\left(\nu + \frac{\nu_t}{\sigma_t}\right)\frac{\partial\tilde{\nu}_t}{\partial x_j}\right) - C_{r1}\frac{\partial\tilde{\nu}_t}{\partial x_j}\frac{\partial\tilde{\nu}_t}{\partial x_j} + C_{r2}\frac{\tilde{\nu}_t}{k}\frac{\partial\tilde{\nu}_t}{\partial x_j}\frac{\partial k}{\partial x_j} - C_{r3}\left(\frac{\tilde{\nu}_t}{k}\right)^2\frac{\partial k}{\partial x_j}\frac{\partial k}{\partial x_j} \tag{13}$$

where C with different subscripts are model coefficients whose values are given in the next subsection.

The modeling assumption leading to Eq. (13) is in part asymptotically inconsistent as a solid wall is approached. The modeled destruction term Π_ε in Eq. (11), for example, has not followed the analysis as in the derivation of LRN k–ε models, where an empirical function, $f_2 = \mathcal{O}(y^2)$ as $y \to 0$, has often been multiplied to $C_{\varepsilon 2}$ so that $\Pi_\varepsilon \propto y^0$. Note that the modeled $\tilde{\nu}_t$ equation (13) yields an asymptotic relation of $\tilde{\nu}_t \propto y$ as $y \to 0$. Such a linear limiting behavior was also argued to hold in the Baldwin–Barth model[9] and the Spalart–Allmaras model.[7] The balance of $\tilde{\nu}_t$ on the wall surface is then established with the involvement of the viscous diffusion and the cross-diffusion terms. This will be further shown in the computation of channel flow.

We want to make the model appropriate to simulating wall-bounded flows when directly integrating it towards the wall surface. It is then necessary to assure a correct eddy viscosity ν_t in the vicinity of the wall surface, which requires that $\nu_t \propto y^3$ as $y \to 0$. Instead of introducing empirical functions into the model equation to account for viscous and wall damping effects, this is achieved by directly modifying $\tilde{\nu}_t$ itself in the viscous sublayer through a damping function f_μ. In a way similar to that used in some previous one-equation models,[7,9,10] the true corrected eddy viscosity ν_t is then calculated from

$$\nu_t = f_\mu\tilde{\nu}_t \tag{14}$$

Retaining the linear asymptotic behavior for $\tilde{\nu}_t$ close to the wall surface, we should then have $f_\mu \propto y^2$ as $y \to 0$. This empirical function has been devised pragmatically as

$$f_\mu = \left[1 - e^{-(R_t/11)}\right]^2\left[1 - 0.9e^{-(R_t/16.5)^4}\right] \tag{15}$$

To close the system of the governing equations, it is necessary to determine the turbulent kinetic energy k appearing in the $\tilde{\nu}_t$ equation. One way to achieve this is to use the Bradshaw assumption,[8] as done in Menter's one-equation model.[10] This will consequently introduce the von Kármán length scale into Eq. (13) to eliminate the k-related terms, making the equation system very complicated and numerically stiff. On the other hand, it is desirable for the model to be applicable for computing complex internal flows, where the availability of the Bradshaw relation[8] is not well calibrated. Moreover, in many practical applications, the solution of turbulent kinetic energy is useful, for example, for estimating the draught risk in a ventilation flow system. We have, therefore, abandoned the formation of a one-equation model and kept the turbulence kinetic energy as a supplemental quantity leading to a two-equation closure. As in other RANS models based on the k equation, this equation is readily modeled by replacing the dissipation term with a relation of $\varepsilon = C_k k^2/\tilde{\nu}_t$. It reads

$$\frac{\mathrm{D}k}{\mathrm{D}t} = \tau_{ij}\frac{\partial U_i}{\partial x_j} - C_k\frac{k^2}{\tilde{\nu}_t} + \frac{\partial}{\partial x_j}\left(\left(\nu + \frac{\nu_t}{\sigma_k}\right)\frac{\partial k}{\partial x_j}\right) \tag{16}$$

Note that the dissipation and diffusion terms modeled in Eq. (16) are not appropriately subjected to near-wall asymptotic requirements. This will render these modeled terms inconsistent with their exact counterparts in the vicinity of a wall surface, yielding a linear

near-wall asymptotic behavior for k. The balance of the k equation will consequently be retained in a way somewhat similar to that of Wilcox's k–ω model, where the dissipation and diffusion of k approach zero on the wall surface.[16] A remedy to this flaw is to multiply a damping function to C_k to force the dissipation term to be asymptotically proportional to y^0 as the wall is approached. However, without there being any significant consequences in the prediction for the mean flow, it is not necessary to construct a model more sophisticated than the present one. This is due to the k equation being a supplemental one in the present two-equation model, and the true ν_t not being directly formulated in terms of k and another scale-determining quantity (e.g., ε or ω) as in other types of two-equation models. As argued, the near-wall limiting behavior of ν_t has been corrected through the damping function f_μ. The turbulent shear stress will consequently possess a correct near-wall asymptotic property, as desired.

The model coefficients raised in the k and $\tilde{\nu}_t$ equations are established in the following subsection.

B. Model Constants

The present model contains eight constants that must be determined for numerical implementation. Some of the constants may be established by manipulation of the coefficients from the corresponding terms in the k–ε model during the transformation, as shown in Eqs. (10) and (11). If we let $\tilde{\nu}_t = C_\mu k^2/\varepsilon$, as with the high-Reynolds-number k–ε model, it will yield $C_k = C_\mu$, $C_1 = (2 - C_{\varepsilon 1})$ and $C_2 = C_\mu(2 - C_{\varepsilon 2})$.

Note that the $\tilde{\nu}_t$ equation has a physical mechanism of describing turbulence transport that is different from the scale-determining equation in other two-equation models, such as the ε equation and the ω equation. Instead, its physical rationale is similar to that of the k equation. Both the quantities of k and $\tilde{\nu}_t$ represent the turbulence level, whereas $\tilde{\nu}_t$ is also able to indicate the ability of a turbulent flow to transport momentum. It is, thus, expected that these two equations will have closely corresponding behavior in describing fully developed turbulence. It is desirable and possible to calibrate the model constants using some classical arguments within the context of two-equation turbulence models.

We consider first decaying, isotropic turbulence. Experiments suggest that the turbulent kinetic energy decays with time following a relation of $k \sim t^{-p}$ with $p \approx 1.2$–1.3. The k and $\tilde{\nu}_t$ equations in this case become

$$\frac{\mathrm{d}k}{\mathrm{d}t} = -C_k \frac{k^2}{\tilde{\nu}_t} \tag{17}$$

$$\frac{\mathrm{d}\tilde{\nu}_t}{\mathrm{d}t} = -C_2 k \tag{18}$$

The asymptotic solution for k obtained from Eqs. (17) and (18) is $k \sim t^{-C_k/(C_k - C_2)}$. This implies that $C_k/(C_k - C_2) = p$. Using the experimental observation gives

$$C_2/C_k = (p-1)/p = 0.167 - 0.23 \tag{19}$$

The model coefficient, on the other hand, should render the model a solution consistent with the law of the wall for a local-equilibrium boundary layer in the absence of a pressure gradient. In the log layer, the eddy viscosity ν_t equals $\kappa u_\tau y$. This suggests

$$\tilde{\nu}_t = \frac{\kappa u_\tau y}{f_{\mu(R_t \to \infty)}} \tag{20}$$

where κ is the von Kármán constant and $\kappa = 0.41$. Together with Eq. (20), it is an easy matter to verify that the model possesses the following solution in the log layer, namely,

$$\frac{\mathrm{d}U}{\mathrm{d}y} = \frac{u_\tau}{\kappa y}, \qquad k = \frac{u_\tau^2}{\sqrt{f_{\mu(R_t \to \infty)} C_k}} \tag{21}$$

As it is defined, $\tilde{\nu}_t$ should approach the true eddy viscosity when the flow is fully developed turbulence. That is, $\tilde{\nu}_t \to \nu_t$ as $R_t \to \infty$. The model function f_μ [see Eq. (15)] has been devised in such a way that $f_{\mu(R_t \to \infty)} = 1$ to meet this condition. In accordance with experimental measurements, $u_\tau^2/k \approx 0.3$. This gives $C_k = 0.09$ from Eq. (21). To make the modeled $\tilde{\nu}_t$ equation satisfy the log law, in addition, the following relation must hold true:

$$C_1 = C_2/C_k - \kappa^2/\sigma_t\sqrt{C_k} + C_{r1}\kappa^2/\sqrt{C_k} \tag{22}$$

The preceding arguments have imposed some guidelines on the establishment of the model coefficients that we have followed to assure the model of correct behavior for some simple fundamental turbulent flows as considered earlier. The coefficients have been further calibrated and optimized in numerical simulations for complex flows. Their values are established as follows:

$$C_k = 0.09, \quad C_1 = 0.4, \quad C_2 = 0.018, \quad C_{r1} = 1.2$$
$$C_{r2} = 1.17, \quad C_{r3} = 0, \quad \sigma_k = 1.2, \quad \sigma_t = 1.2 \tag{23}$$

Equations (13–16), together with the model constants in Eq. (23), form the present two-equation model. Note that an ε equation can be obtained by a transformation using the present k and $\tilde{\nu}_t$ equations. The transformed ε equation will consequently give model constants $C_{\varepsilon 1} = 1.6$ and $C_{\varepsilon 2} = 1.8$ for the production term and the destruction term, respectively, compared with $C_{\varepsilon 1} = 1.44$ and $C_{\varepsilon 2} = 1.92$ in the conventional k–ε model. Owing to the diffusion operator, in addition, the resultant ε equation includes extra cross-diffusion terms that are similar to those in Yoshizawa's model derived from the two-scale direct-interaction approximation.[17] The role played by such cross-diffusion terms was investigated by Yoon and Chung[18] in computations of compression ramp flows. It was claimed that these terms are able to improve the prediction of skin friction for such nonequilibrium flows.

III. Numerical Results

Four cases are considered in this section to validate the present two-equation model. These include a channel flow, a channel flow over a two-dimensional hill mounted on the bottom wall, and two backward-facing step flows at a low and a high Reynolds number. The numerical results are compared with experimental and DNS data.

The model equations were numerically approximated using the finite volume method. The convective derivatives were discretized by the third-order upwind biased differencing scheme QUICK, and the central differencing scheme was used for other terms. The SIMPLEC algorithm was used to deal with the velocity–pressure coupling. The boundary-fitted coordinate system was employed, and the grid system was nonstaggered.[19] For all of the flow cases considered, the grid used was nonuniform with clustered nodes near the wall to resolve the sharp gradient. The grid resolution was carefully investigated to confirm grid-independent solutions. The solution convergence was ascertained until the normalized residual for all of the computed variables dropped below the level of 10^{-4}.

The present model renders a natural condition for $\tilde{\nu}_t$ at the wall. The boundary conditions for the mean velocities and turbulent quantities are all zero on the wall surface, that is, $U = V = k = \tilde{\nu}_t = 0$. The boundary condition at the inlet section is prescribed according to the experimental data or DNS data. For cases in which inflow data are not available for some quantities, estimated or precalculated profiles are used as stated hereafter. Neumann conditions have been employed at the outlet for all cases.

A. Channel Flow

Fully developed turbulent channel flows are attractive for model validation because they have self-similar solutions that do not depend on the inlet and initial conditions as the flow is fully developed. On the other hand, the effect of the wall on turbulent shear flow is present, requiring justified representation in the model to account for near-wall turbulent transport. In this work, computations are carried out for a two-dimensional fully developed channel flow at $Re_\tau = 3.95 \times 10^2$, for which DNS data are available.[20]

Figure 1 shows the distributions of the computed mean velocity, turbulent kinetic energy, and turbulent shear stress. In Fig. 1a, U_c is the centerline velocity. The results are compared with the DNS data and with the results obtained from the Abe et al. LRN k–ε

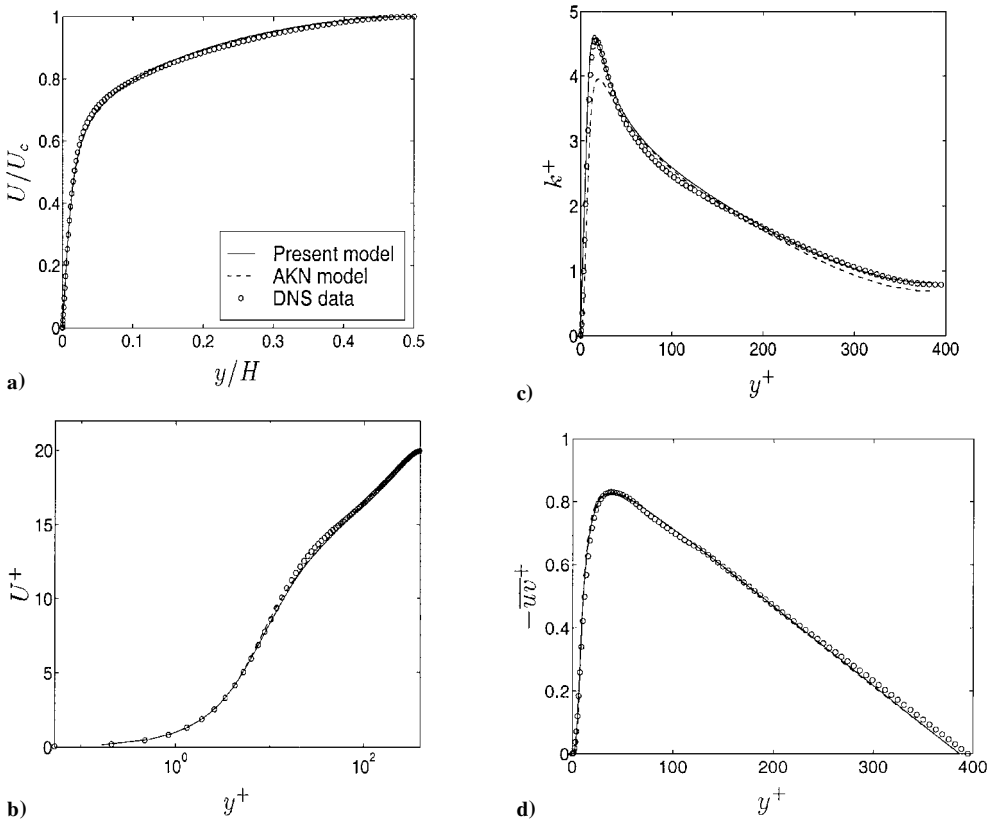

Fig. 1 Predictions for channel flow at $Re_\tau = 3.95 \times 10^2$.

model[21] (hereafter the AKN model). Both models yield predictions for the mean velocity and turbulent shear stress that are in satisfactory agreement with the DNS data. In comparison with the DNS data and the prediction reproduced by the present model, the AKN model underpredicts the near-wall peak of turbulent kinetic energy by about 15%.

The eddy viscosity in the present model has been computed through a transport equation. It is desirable to compare this quantity with the DNS result. The DNS eddy viscosity is calculated here from $\nu_{t\text{DNS}} = -\overline{uv}/(\partial U/\partial y)$. In Fig. 2a, the distribution of the eddy viscosity computed from the model is compared with the DNS result in a log–log plot. The model replicates the asymptotic behavior of ν_t that is identical to the DNS data, suggesting that the slope of the near-wall curve for (ν_t/ν) in the log–log plot is 3, that is, $\nu_t \propto y^3$. In Fig. 2b, the budget for the k equation is illustrated in comparison with the DNS data. As can be seen, both the dissipation term and the diffusion term in the viscous sublayer possess a different tendency from the corresponding DNS profiles and approach zero on the wall surface. The production term, by contrast, fits very well with the DNS result all of the way to the wall. Away from the viscous sublayer, all of the terms in the budget are in reasonable agreement with the DNS data. The near-wall behavior nestled in the present k equation is somewhat similar to that in the standard k–ω model[16] but renders a generally better prediction for the turbulent kinetic energy away from the wall. As a whole, the dissipation term, $\varepsilon = C_k k^2/\tilde{\nu}_t$, in the k equation is proportional to y^1 as $y \to 0$, entailing no singularity problem in numerical implementation. On the other hand, note that the asymptotic behavior of this term can be corrected by modifying model coefficient C_k through an additional empirical function f_k. As mentioned, however, the turbulent kinetic energy in the present two-equation model is a supplemental quantity to the $\tilde{\nu}_t$ equation. Now that the asymptotic property for the true eddy viscosity ν_t is assured, as shown in Fig. 2a, no significant consequence should be caused in the mean flow computation using this model.

The near-wall modeling approach adopted in the present k equation will consequently give rise to asymptotic behavior of $k \propto y$ as $y \to 0$, although a correct prediction of k beyond $y^+ = 10$ is

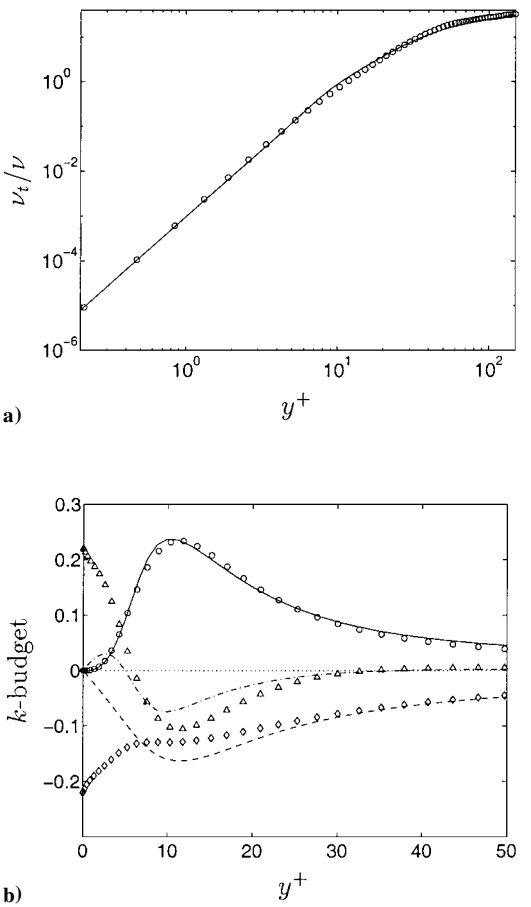

Fig. 2 Channel flow computation with the present model: a) near-wall distribution of the true eddy viscosity ν_t and b) budget of the k equation in which the lines represent the model predictions and the symbols are the DNS data: ∘, production; ◇, dissipation; and △, diffusion.

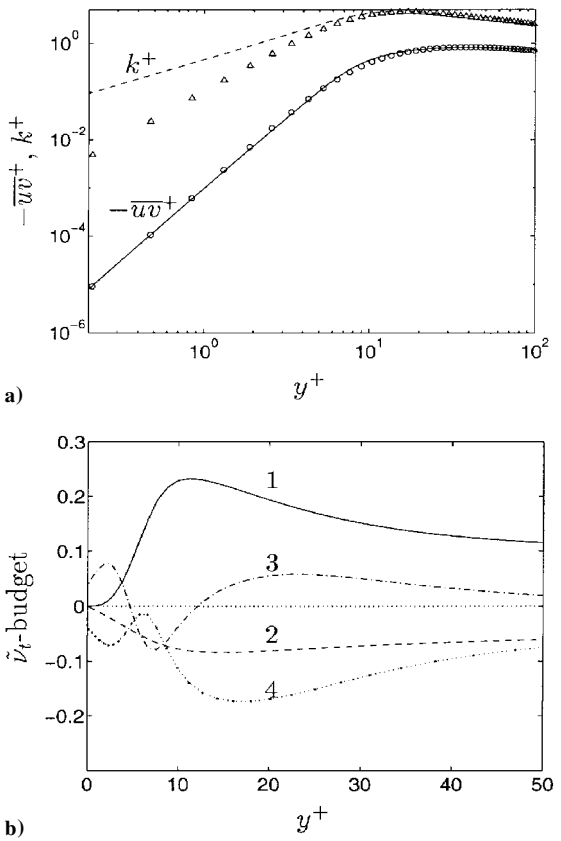

Fig. 3 Channel flow computation with the present model: a) near-wall distributions of $-\overline{uv}^+$ and k^+ and b) budget of the $\tilde{\nu}_t$ equation in which 1 is the production, 2 is the destruction, 3 is the second-order diffusion, and 4 is the total cross diffusion; ($T_{r1} + T_{r2}$).

obtained. This is illustrated in Fig. 3a. Also shown in this log–log plot is the near-wall distribution for $-\overline{uv}^+$, which displays an asymptotically correct property, $-\overline{uv} \propto y^3$, in the viscous sublayer. Figure 3b plots the budget of the $\tilde{\nu}_t$ equation. Consistent with the near-wall behavior of $\tilde{\nu}_t \propto y$, the two first-order diffusion terms, multiplied by constants C_{r1} and C_{r2} in Eq. (13) and denoted hereafter as cross-diffusion terms T_{r1} and T_{r2}, respectively, are proportional to y^0 as $y \to 0$. It is shown that the balance on the wall surface is established by the viscous diffusion and the cross-diffusion terms ($T_{r1} + T_{r2}$), whereas the production term and the destruction term approach zero. Note that the last cross-diffusion term in Eq. (13) is excluded by setting $C_{r3} = 0$. Also note that, near the wall, the cross-diffusion terms are of opposite signs and $|T_{r1}| + |T_{r2}| \gg T_{r1} + T_{r2}$.

The reasonable prediction of ν_t and $-\overline{uv}$ in the near-wall region suggests that the viscous and wall damping effects on the mean flow have been appropriately accounted for. It indicates the appropriateness of the present model as integrated over the near-wall region. However, reasonable caution should be exercised in a priori testing of the model using DNS data because of the inconsistent near-wall behavior of k. As noted, to achieve a precise k distribution in the viscous sublayer, an empirical function must be used to modify the dissipation term in the k equation, which may resort to a priori testing using DNS data.

B. Channel Flow over a Two-Dimensional Hill

This case concerns the flow over a single hill mounted on the bottom wall of a plane channel. The maximum height of the hill is $h = 28$ mm, and the length is 108 mm. The ratio between the hill height and the channel height H is 6.07. The Reynolds number based on h and the upstream central line velocity is 6×10^4. The experiment was carried out by Almeida et al.[22] A recirculation zone is present on the lee slope, extending from about $0.43h$ to $4.82h$ downstream of the hill summit. The measurement was made in the vertical center plane of the tunnel, which is 200 mm wide (compared to the height of 170 mm). Some deviations from the two dimensionality of this flow in this plane cannot be ruled out, even though this has been assumed in the calculation.

The computational domain covers a length of about $3.6h$ upstream and $18h$ downstream of the hill summit. A boundary-fitted, structured mesh with 130×100 cells is used for the flow resolution. The grid is stretched in the near-wall region, generally giving $y^+ < 1$ for the first node close to the wall surface. To confirm the grid independence of the reported results, a calculation was carried out with a doubled grid (260×200 cells). The variation between the results obtained using the two grids was virtually identical, disclosing grid-independent solutions.

The inflow conditions are adopted from the measurement data. However, the $\tilde{\nu}_t$ distribution is not available from the experiment. This has been estimated through an approximation: $\varepsilon_{\text{in}} = C_k^{3/4} k_{\text{in}}^{3/2} / L$ and $L = (\kappa y \cdot l_H)/(\kappa y + l_H)$ with $l_H = H/4$, and $\tilde{\nu}_{t\,\text{in}} = C_k k_{\text{in}}^2 / \varepsilon_{\text{in}}$, where y is the closest distance to the walls. Note that the predicted distributions are found to be rather insensitive to the choice of l_H, which may, however, cause a slight variation in the reattachment length X_r. A change from $l_H = H/4$ to $l_H = H/10$ may alter X_r by about 6%.

Figure 4a shows the geometry and the grid used. The streamline contour computed by the present model is illustrated in Fig. 4b. The reattachment lengths predicted by the AKN model and the present model are nearly the same, with a value of $(4.85 - 4.9)h$, which is very close to the experimental observation.

This flow was a test case during a European Research Community on Flow, Turbulence and Combustion/International Association for Hydraulic Research (ERCOFTAC/IAHR) workshop,[23] where more than 30 groups of results were compared using various RANS approaches including the standard k–ε model with wall functions, LRN and RNG k–ε and k–ω models and Reynolds stress models. It was noted that entirely satisfactory agreement with experiments could not be achieved with any model used at that workshop. For the mean flow quantities, even the more complex models did not show better performance than the simpler linear eddy viscosity models.

Figure 5 shows the distributions of U, V, k, and $-\overline{uv}$ at four different positions downstream of the hill summit, $x/h = 1.0714$, 3.214, 4.786, and 6.607.

The models give somewhat similar results for this case. In comparison with the experimental data, the present model reproduces

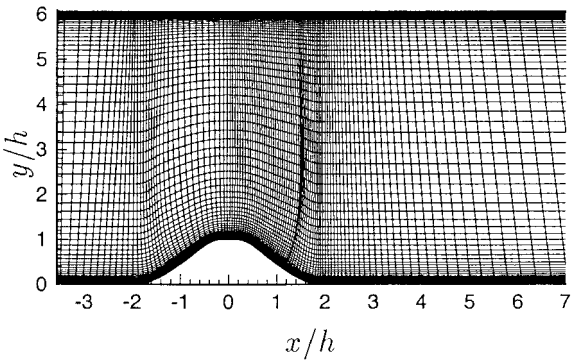

a) Geometry and grid

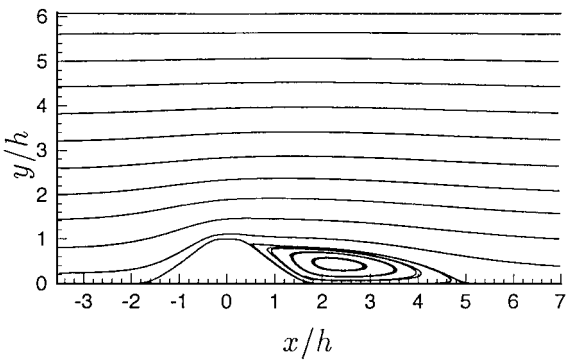

b) Streamline contour

Fig. 4 Channel flow over a hill.

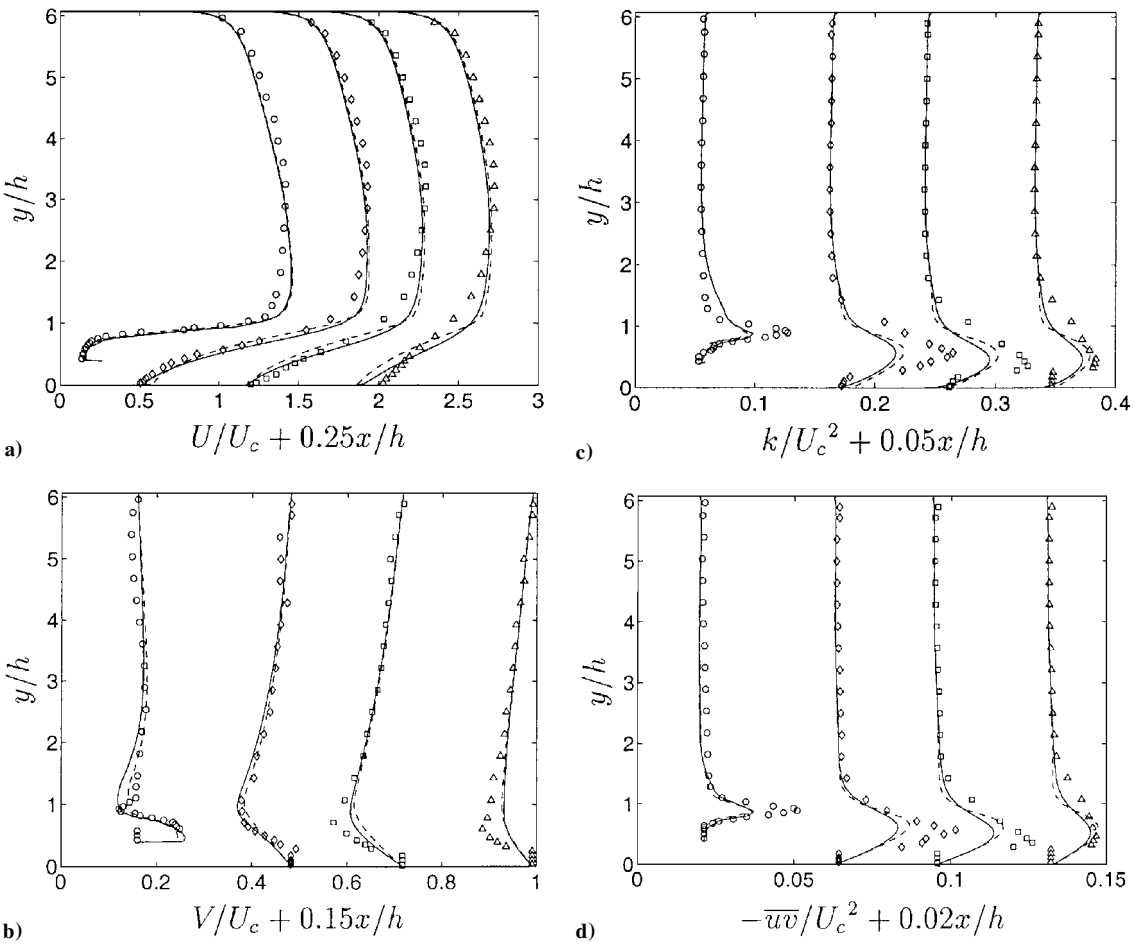

Fig. 5 Computed distributions for flow over a hill in a plane channel at $x/h = 1.0714$ (○), $x/h = 3.214$ (◇), $x/h = 4.786$ (□), and $x/h = 6.607$ (△); ——, present model, and - - - -, AKN model.

slightly better distributions for the mean streamwise velocity than does the AKN model near the bottom wall where the hill is mounted (see Fig. 5a). Both models underpredict the peaks for k and $-\overline{uv}$ in the recirculation bubble, showing an underestimation of turbulence intensity in this region. These peaks, however, tend to gradually approach the experimental profile downstream of the reattachment point. Also underpredicted is the vertical velocity V at and after the reattachment point, where the mean streamwise velocity also shows too slow a recovery as compared to the measured profile, particularly with the AKN model. The flow inside the separation bubble is characterized by strongly anisotropic turbulence. The inaccurately predicted turbulence level in this region may largely be attributed to the models used which, by their linear nature, are unable to appropriately respond to strong anisotropy. Moreover, the slow-recovery problem downstream of the massive separation generally exists for separating and reattaching flows at high Reynolds numbers when using linear eddy viscosity models and even some stress models, as pointed out in some previous studies.[10,24,25] This phenomenon also exists in the backward-facing step flow computations at high Reynolds numbers, as shown in the next subsection. The underprediction of the near-wall peaks for k and $-\overline{uv}$ as reported here was also generally seen in the RANS models used at the ERCOFTAC/IAHR workshop. The present model is able to give similar or improved predictions as compared with the results presented in that workshop.[23]

C. Backward-Facing Step Flow

The flow over a backward-facing step has commonly been used in the validation of turbulence models, on which the nonequilibrium effect is calibrated in the presence of adverse pressure gradient and flow separation. The model is applied to two backward-facing step flows in this subsection. These include the flow by Le et al.[26] (hereafter the LMK case), who carried out a direct numerical simulation, and the flow experimentally studied by Driver and Seegmiller[27] (hereafter the DS case). The computations were performed on a grid containing 192×182 cells for the LMK case and a 205×212 grid for the DS case. Substantial grid refinement near the step and wall surfaces has been made to reproduce near-wall resolutions. The inlet section profiles were taken from the DNS data for the LMK case and from the measurements for the DS case. The inflow eddy viscosity was computed for both cases from $\tilde{\nu}_t = C_k k_{\text{in}}^2/\varepsilon_{\text{in}}$ and $\varepsilon_{\text{in}} = \mathcal{P}_k = -\overline{uv}(\partial U/\partial y)$ at the inlet section.

In the LMK case, the Reynolds number Re, based on the step height h and the freestream velocity U_c, is 5.1×10^3, and the expansion ratio is 1.2. The upstream Reynolds number based on the momentum thickness is $Re_\theta = 6.7 \times 10^2$, and the boundary-layer thickness is $\delta = 1.2h$. The numerical domain covers $10h$ upstream and $30h$ downstream of the step. In Fig. 6, the model predictions are compared with the DNS data at six positions ($x/h = 0$ located at the step). Both the present model and the AKN model yield generally reasonable predictions as compared with the DNS profiles. They predict nearly identical distributions for the mean streamwise velocity, with the exception that the AKN model predicts slightly smaller magnitudes near the bottom wall inside the separation bubble (Fig. 6a). After the reattachment point, the streamwise velocity recovers properly to a boundary-layer profile, as desired. The present model is able to give better predictions for the turbulent kinetic energy than the AKN model downstream of the step, but it slightly underpredicts the turbulent shear stress. In addition, this model shows a somewhat better response in the curved spreading shear layer in the prediction of the turbulent quantities than does the AKN model.

With regards to the reattachment length, the DNS gives $X_r = 6.28h$ downstream of the step. The AKN model underpredicts this value by about 10%, giving $X_r = 5.65h$, and the present model

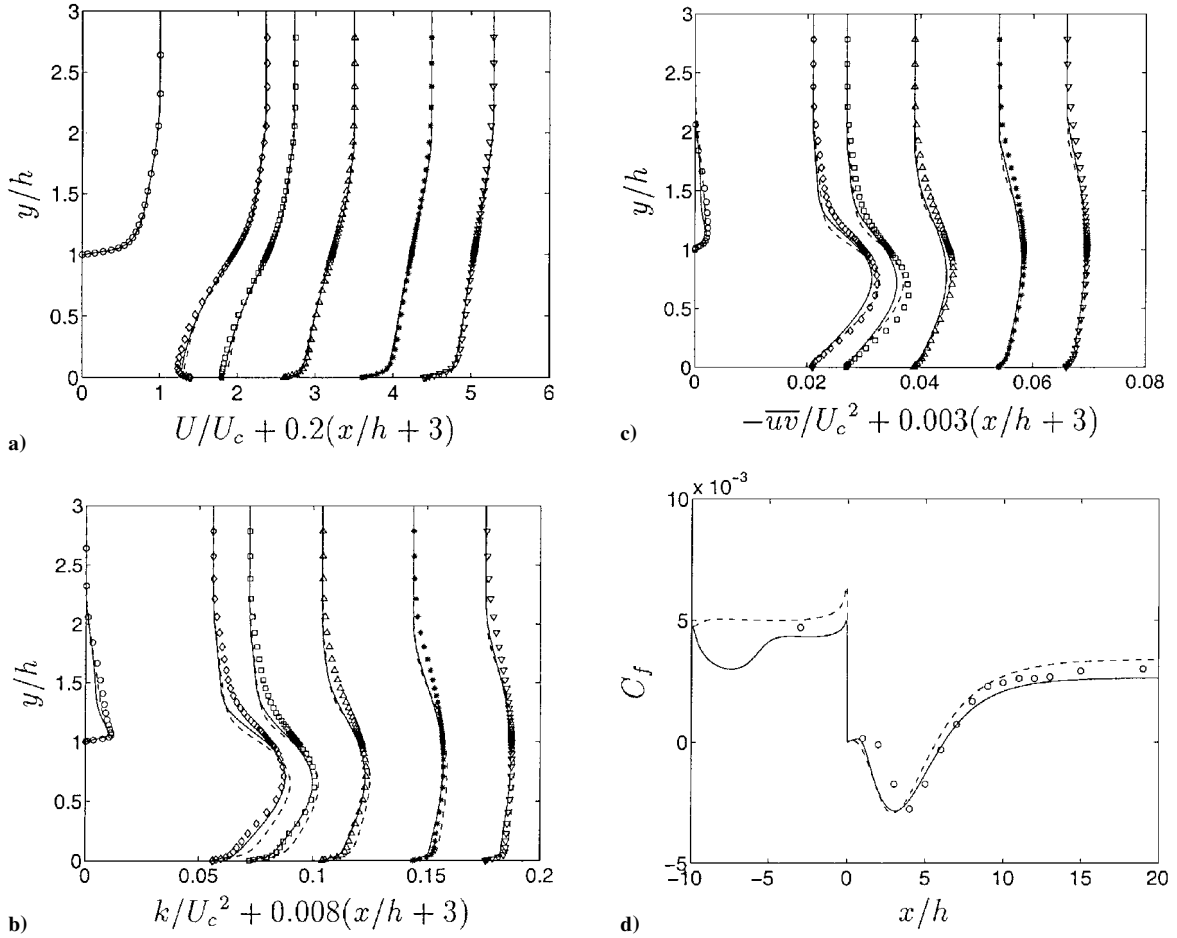

Fig. 6 Computed distributions for backward-facing step flow (LMK case[26]) at $x/h = -3$ (∘), 4 (◇), 6 (□), 10 (△), 15 (∗), and 19 (∇); ——, present model, and - - - -, AKN model.

predicts $X_r = 6.22h$. The distribution of the skin-friction coefficient C_f along the bottom wall is shown in Fig. 6d. The C_f value given by the present model first drops and then recovers to a flat level similar to the DNS value after a distance of about $5h$ from the inflow section. This is due to the inflow specification for the eddy viscosity $\tilde{\nu}_t$, which does not appropriately match the model equations to reproduce the upstream boundary-layer profile as obtained in the DNS. This should not cause any effects in the prediction, however, because the boundary-layer velocity profile has been well recovered at a distance of (4–5)h upstream of the step, as seen from the velocity distribution at $x/h = -3$ in Fig. 6a. Figure 6d also shows that both models return too intensive a backflow inside the recirculation bubble approaching the step wall. This consequently squeezes the secondary corner bubble below the step. The underestimation of the secondary corner bubble is a phenomenon encountered in computations even with higher-order RANS closures.[25,28]

The DS case allows a test of the model in a high-Reynolds-number configuration. The Reynolds number, defined as in the LMK case, is $Re = 3.75 \times 10^4$, and the expansion ratio is 1.125. Measurements were made using laser velocimetry. Upstream of the step, the wall boundary-layer thickness is $\delta = 1.5h$, and the Reynolds number based on the momentum thickness is $Re_\theta = 5 \times 10^3$. The numerical domain for this case covers a length of $4h$ upstream and $40h$ downstream of the step.

The model predictions are given in Fig. 7 in comparison with the experimental data. Both the present model and the AKN model reasonably reproduce the mean streamwise velocity in the recirculation region but severely fail to recover the boundary-layer profile downstream of the reattachment location (Fig. 7a). The same experience has been reported in computations using other RANS models.[25,28] The prediction for the turbulent kinetic energy and shear stress agrees reasonably well with the experimental data except in a narrow region inside the separation bubble (at $x/h = 4$ and 6, respectively), where the peaks of k and $-\overline{uv}$ are underpredicted and move up from the region near the bottom wall (Figs. 7b and 7c). Similar results for this flow were also reported when using other RANS models.[24,25] Moreover, note that the present model yields somewhat better predictions for k and $-\overline{uv}$ in the spreading shear layer above the recirculation bubble, as is also illustrated for the LMK case.

The experiment observed a reattachment length of $X_r = 6.26h$ downstream of the step. The AKN model predicts a value of about $6.12h$, which agrees well with the measured data. The present model overpredicts this quantity by about 9%, giving $X_r = 6.85$. The skin-friction coefficient along the bottom wall is underpredicted by the present model after the reattachment, whereas the AKN model overpredicts this quantity in a narrow range in the recovery region. Note that this quantity predicted by the AKN model is brought to the same level as that arrived at by the present model in the recovery region after about $x/h = 30$ from the step. Moreover, the overpredicted C_f (negative values) in the separation bubble indicates that the models have overestimated the backflow and stretched the secondary corner bubble so that the negative dip of the computed C_f starts too close to the step.

One of the main purposes of this work is to show the performance of a two-equation model when coupling an eddy-viscosity transport equation with the turbulent kinetic energy equation. In general, this model shows a satisfactory capability for dealing with near-wall turbulence transport. On the other hand, some inaccurate behavior was also found in predicting backward-facing step flows at different Reynolds numbers. The apparent difference in this case is the predictions of the reattachment length and the recovery region. At a low Reynolds number (e.g., for the LMK case) reasonable results can be obtained. Applied to the flow at a high Reynolds number

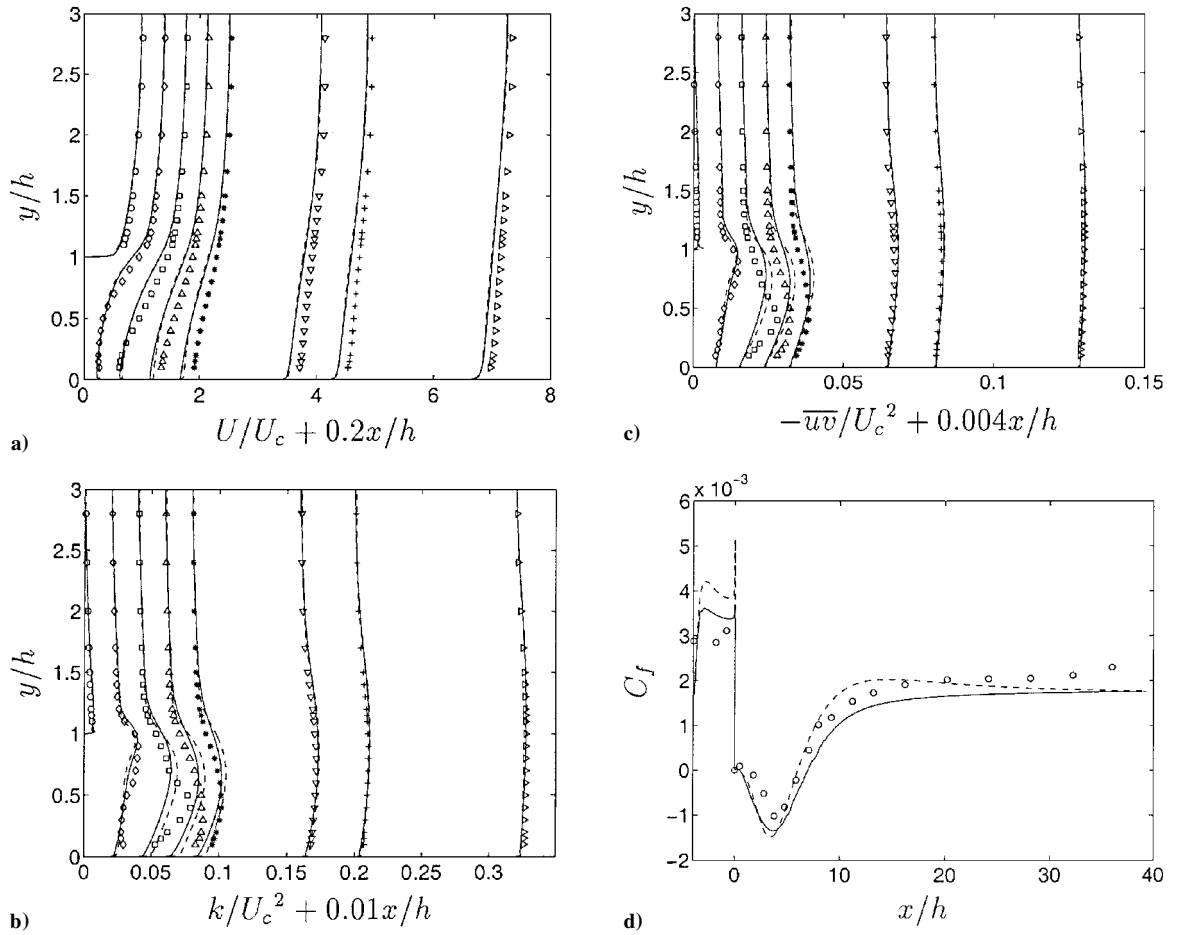

Fig. 7 Computed distributions for backward-facing step flow (DS case[27]) at x/h = 0 (∘), 2 (◇), 4 (□), 6 (△), 8 (∗), 12 (▽), 20 (+), and 32 (.); ——, present model, and - - - -, AKN model.

(e.g., the DS case), the model somewhat overestimates the size of the separation bubble, and the streamwise velocity recovers too slowly to a boundary-layer profile downstream of the reattachment point. Similar phenomena were also identified in previous studies using Reynolds stress models and other RANS models.[24,29,30] The velocity-recovery problem does not seem to stem from the near-wall treatment. Instead, it may be caused by the RANS modeling frame.

With no loss of the accuracy in the channel flow prediction, effort has been made to observe the influence of the model coefficients on the separated flow computations. It was found that the constants for the two cross-diffusion terms in the $\tilde{v}_t$ equation (i.e., C_{r1} and C_{r2}) have little effect on the results, provided that the difference between these terms remains at a certain level. Constants C_1 and C_2, however, may trigger a significant influence on the predictions. An increase in C_1 or decrease in C_2 will reduce the reattachment length and vice versa. The value of C_2 possesses a narrow range for tuning if we are willing to keep the limitation imposed by Eq. (19) for computing isotropic turbulence decay. Using $C_2 = 0.018$ and increasing C_1 from 0.4 to about 0.45 may render a reattachment length that fits well with the measured data in the DS flow computation but underpredicts this quantity by more than 15% for the LMK case. Such a tuning gives no significant improvement in the mean flow prediction for the DS case, except that the velocity in the recovery region becomes slightly closer to the measured profiles because the downstream recovery starts earlier in this case. On the other hand, the turbulent quantities, k and $-\overline{uv}$, deviate more from the measurements and become larger than the results reported here, particularly in the spreading shear layer. For the LMK case, the tuning may improve the predictions for k and $-\overline{uv}$ in spite of the underprediction of the reattachment length. Nonetheless, the negative backflow velocity inside the separation bubble is underpredicted near the bottom wall (although the velocity profiles downstream of the reattachment point are reproduced well).

IV. Conclusions

This work presented a linear two-equation model for turbulent flow computations. Instead of constructing the eddy viscosity from the scale-determining turbulent quantities, a transport equation for the eddy viscosity is proposed. This equation is modeled on the basis of an exact form transformed from the exact k and ε equations. As in nearly all existing two-equation closures, the turbulent kinetic energy equation is also solved in this two-equation model, but functions only as a supplemental quantity to eliminate the k-related terms in the eddy-viscosity transport equation to close the equation system. The model allows the integration of the equation to the wall surface, requiring neither wall functions as a bridge to patch the near-wall region nor wall distance parameters in the model coefficients.

The model was applied to fully developed channel flow, channel flow with a hill mounted on the bottom wall, and backward-facing step flow. The predictions were compared with the DNS and experimental data, showing generally reasonable performance. With a relatively simple equation system and only one empirical damping function free of wall parameters, the present model shows a very good capability for near-wall treatment in dealing with wall damping and viscous effects on the mean flow. This model appears to be a worthwhile alternative approach to other high-Reynolds-number and LRN eddy-viscosity models when computing complex turbulent flows where the near-wall region is of importance in the simulation.

Being a linear eddy-viscosity model, on the other hand, it is unavoidable for the proposed model to retain some common deficiencies stemming from Boussinesq's assumption generally existing in other two-equation models. It is well known that the linear gradient-diffusion hypothesis is not universally applicable for separating and reattaching flows with strong anisotropy. The use of such a hypothesis is practically simple but may render undesirable disadvantages as compared with some nonlinear and higher-order

RANS approaches. Nonetheless, the main purpose here is to present an alternative two-equation model and to validate its performance for computing nonequilibrium flows. The work has shown that this model is capable of yielding similar or better predictions as compared with other existing two-equation models, while having some advantages, as mentioned, such as the natural boundary condition at the wall and in the far field for $\tilde{\nu}_t$ and wall-distance free model coefficients. Further work will be carried out to enhance the present linear model to a nonlinear form for simulating turbulent flows with strong anisotropy.

References

[1]Patel, V., Rodi, W., and Scheuerer, G., "Turbulence Models for Near-Wall and Low Reynolds Number Flows: A Review," *AIAA Journal*, Vol. 23, No. 9, 1985, pp. 1308–1319.

[2]Wilcox, D., "Simulation of Transition with a Two-Equation Turbulence Model," *AIAA Journal*, Vol. 32, No. 2, 1994, pp. 1192–1198.

[3]Peng, S.-H., Davidson, L., and Holmberg, S., "A Modified Low-Reynolds-Number $k-\omega$ Model for Recirculating Flows," *Journal of Fluids Engineering*, Vol. 119, Dec. 1997, pp. 867–875.

[4]Speziale, C., Abid, R., and Anderson, E., "Critical Evaluation of Two-Equation Models for Near-Wall Turbulence," *AIAA Journal*, Vol. 30, No. 2, 1992, pp. 324–331.

[5]Baldwin, B., and Lomax, H., "Thin-Layer Approximation and Algebraic Model for Separated Turbulent Flows," AIAA Paper 78-257, Jan. 1978.

[6]Johnson, D. A., and King, L. S., "Mathematically Simple Closure Model for Attached and Separated Turbulent Boundary Layers," *AIAA Journal*, Vol. 23, No. 11, 1985, pp. 1684–1692.

[7]Spalart, P. R., and Allmaras, S. R., "One-Equation Turbulence Model for Aerodynamic Flows," AIAA Paper 92-0439, Jan. 1992.

[8]Bradshaw, P., Ferriss, D., and Atwell, N., "Calculation of Boundary-Layer Development Using the Turbulent Energy Equation," *Journal of Fluid Mechanics*, Vol. 28, Pt. 3, 1967, pp. 593–616.

[9]Baldwin, B. S., and Barth, T. J., "One-Equation Turbulence Transport Model for High Reynolds Number Wall-Bounded Flows," AIAA Paper 91-0610, Jan. 1991.

[10]Menter, F. R., "Eddy Viscosity Transport Equations and Their Relation to the $k-\varepsilon$ Model," *Journal of Fluids Engineering*, Vol. 119, Dec. 1997, pp. 876–884.

[11]Wilcox, D., *Turbulence Modeling for CFD*, DCW Industries, La Cañada, CA, 1993.

[12]Nee, V. W., and Kovasznay, L. S. G., "Simple Phenomenological Theory of Turbulent Shear Flows," *Physics of Fluids*, Vol. 12, No. 3, 1969, pp. 473–484.

[13]Zeierman, S., and Wolfshtein, M., "Turbulent Time Scale for Turbulent-Flow Calculations," *AIAA Journal*, Vol. 24, No. 10, 1986, pp. 1606–1610.

[14]Abid, R., Speziale, C. G., and Thangam, S., "Application of a New $k-\tau$ Model to Near-Wall Turbulent Flows," AIAA Paper 91-0614, Jan. 1991.

[15]Hinze, J., *Turbulence*, 2nd ed., McGraw–Hill, New York, 1975.

[16]Wilcox, D., "Reassessment of the Scale-Determining Equation for Advanced Turbulence Models," *AIAA Journal*, Vol. 26, No. 11, 1988, pp. 1299–1310.

[17]Yoshizawa, A., "Statistical Modeling of a Transport Equation for the Turbulent Kinetic Energy Dissipation," *Physics of Fluids A*, Vol. 30, No. 3, 1996, pp. 628–631.

[18]Yoon, B. K., and Chung, M. K., "Computation of Compression Ramp Flow with a Cross-Diffusion Modifed $k-\varepsilon$ Model," *AIAA Journal*, Vol. 33, No. 8, 1995, pp. 1518–1520.

[19]Davidson, L., and Farhanieh, B., "CALC-BFC: A Finite-Volume Code Employing Collocated Variable Arrangement and Cartesian Velocity Components for Computation of Fluid Flow and Heat Transfer in Complex Three-Dimensional Geometries," Dept. of Thermo and Fluid Dynamics, Rept. 92/4, Chalmers Univ. of Technology, Gothenburg, Sweden, 1992.

[20]Mansour, N., Kim, J., and Moin, P., "Reynolds-Stress and Dissipation-Rate Budgets in a Turbulent Channel Flow," *Journal of Fluid Mechanics*, Vol. 194, Sept. 1988, pp. 15–44.

[21]Abe, K., Kondoh, T., and Nagano, Y., "A New Turbulence Model for Predicting Fluid Flow and Heat Transfer in Separating and Reattaching Flows—I. Flow Field Calculations," *International Journal of Heat and Mass Transfer*, Vol. 37, No. 1, 1994, pp. 139–151.

[22]Almeida, G. B., Durao, D. F. G., and Heitor, M. V., "Wake Flows Behind Two-Dimensional Model Hills," *Experimental Thermal and Fluid Science*, Vol. 7, 1993, pp. 87–101.

[23]"4th ERCOFTAC/IAHR Workshop on Refined Flow Modelling," *Data Bases and Testing of Calculation Methods for Turbulent Flows*, edited by W. Rodi, J.-C. Bonnin, and T. Buchal, Univ. of Karlsruhe, Karlsruhe, Germany, 1995.

[24]Durbin, P. A., "Separated Flow Computations with the $k-\varepsilon-\overline{v^2}$ Model," *AIAA Journal*, Vol. 33, No. 4, 1995, pp. 659–664.

[25]Michelassi, V., Durbin, P. A., and Mansour, N. N., "Prediction of the Backflow and Recovery Regions in the Backward Facing Step at Various Reynolds Numbers," *Proceedings of the Summer Program 1996*, Center for Turbulent Research, Stanford Univ./NASA Ames Reseach Center, Stanford, CA, 1996, pp. 73–86.

[26]Le, H., Moin, P., and Kim, J., "Direct Numerical Simulation of Turbulent Flow over a Backward Facing Step," *Journal of Fluid Mechanics*, Vol. 330, Jan. 1997, pp. 349–374.

[27]Driver, D. M., and Seegmiller, H. L., "Features of a Reattaching Turbulent Shear Layer in Divergent Channel Flow," *AIAA Journal*, Vol. 23, No. 2, 1985, pp. 163–171.

[28]Parneix, S., Laurence, D., and Durbin, P. A., "A Procedure for Using DNS Databases," *Journal of Fluids Engineering*, Vol. 120, March 1998, pp. 40–47.

[29]Ko, S., "Computation of Turbulent Flow over Backward and Forward-Facing Steps Using a Near-Wall Reynolds Stress Model," *Annual Research Briefs*, Center for Turbulent Research, Stanford Univ., Stanford, CA, 1993, pp. 75–90.

[30]Rodi, W., "Experience with Two-Layer Models Combining the $k-\varepsilon$ Model with a One-Equation Model Near the Wall," AIAA Paper 91-0216, Jan. 1991.

R. M. C. So
Associate Editor